RESEARCH ARTICLE

How certain are El Niño–Southern Oscillation frequency changes in Coupled Model Intercomparison Project Phase 6 models?

Fiona Fix [ORCID] | Stefan A. Buehler [ORCID] | Frank Lunkeit

Universität Hamburg, Hamburg, Germany

Correspondence
Fiona Fix, Meteorologisches Institut, Universität Hamburg, Bundesstrasse 55, 20146 Hamburg, Germany.
Email: fiona.fix@uni-hamburg.de

Abstract

El Niño–Southern Oscillation (ENSO) is one of the most important modes of climate variability on interannual timescales. We aim to find out whether a change in ENSO frequency can be predicted for the nearer future. We analyse the unforced pre-industrial control run and the forced 1%/year CO_2 increase run for an ensemble of 43 general circulation models that participated in the Coupled Model Intercomparison Project Phase 6 (CMIP6). We assume that the uncertainty of ENSO frequency trend estimates from an ensemble is caused by apparent trends as well as model differences. The part of the uncertainty caused by apparent trends is estimated from the pre-industrial control simulations. As a measure for ENSO frequency, we use the number of El Niño- and La Niña-like months in a moving 30-year time window. Its linear decadal trend is calculated for every member. The multimember mean of the trend for both experiments is less than 0.7 events per decade. Given that the standard error is of the same order of magnitude, we consider this a negligible trend. The uncertainties are large in both experiments and we can attribute most of the intermember variability to apparent trends due to natural variability rather than different model reactions to CO_2 forcing. This means that the impact of intermodel differences might have been overstated in previous studies. Apparent trends make it very difficult to make reliable predictions of changes in ENSO frequency based on 120-year time series.

KEYWORDS
climate change, CMIP6, ENSO, ENSO frequency

1 | INTRODUCTION

El Niño–Southern Oscillation (ENSO) is one of the most important modes of climate variability on interannual timescales. Due to teleconnections, it impacts weather conditions worldwide and can lead to extreme weather

events. To reduce the social, economic, and environmental risks of these events, accurate forecasting is required. Therefore, understanding ENSO mechanisms and predicting ENSO events is a central question of current research, especially regarding global warming. Global warming could have different effects on the equatorial Pacific and can therefore affect ENSO in a variety of ways. ENSO frequency can be affected by the sharpness and depth of the equatorial thermocline, the meridional and zonal sea surface temperature (SST) gradients as well as the strength of the trade winds (Timmermann et al., 1999; Yang et al., 2005; Deng et al., 2010). Which one of these influences dominates when it comes to ENSO frequency change, or if there are other processes involved, has yet to be investigated.

There are many studies (e.g., Kestin et al., 1998; Wang and An, 2001; Zhang et al., 2008; Aiken et al., 2013) investigating ENSO dynamics with the help of observations, but it is difficult to conclude how ENSO reacts to climate change. This is because the observational record is short (especially with respect to the timescale of the phenomenon) and ENSO frequency is quite irregular. Also, the ENSO amplitude is large compared to changes in the mean global temperatures; therefore, the variability is large compared to the trend in mean global temperatures. It is well known that to detect a trend of a specific size, a time series of a specific minimum length is needed (or vice versa). How long a time series needs to be so that a trend can be detected depends on the autocorrelation and the variance of the noise in the data (Weatherhead et al., 1998).

To overcome these problems, a longer time series or stronger trend is required. To this end, climate models can be helpful. Experiments can be run for longer times or with increased forcing so that the expected trend is bigger. There are many studies on ENSO frequency change in climate models. Some of them found an increase in ENSO frequency in the models they examined (Timmermann et al., 1999; Collins, 2000b). Collins (2000b), for example, studied ENSO frequency with the second Hadley Centre coupled climate model (HadCM2). The HadCM2 is a coupled climate model which, according to Collins (2000b), represents present-day ENSO conditions (amplitude and frequency) well. By running different climate change scenarios he found that there are only small changes until a quadrupling of CO_2 when the frequency doubles. On the other hand, Yang et al. (2005) investigated ENSO in the Fast Ocean Atmosphere Model and found that a reduction in ENSO frequency is very likely as a result of a warming climate. Yet other studies argued that ENSO frequency does not react to global warming at all (e.g., Timmermann, 2001; Zelle et al., 2005). Also, Collins (2000a) followed up on his

earlier study and found that in the third Hadley Centre coupled climate model (HadCM3) there is no change in ENSO frequency under different climate change scenarios.

Timmermann (2001), Zelle et al. (2005) and Collins (2000a) emphasized the effect that model specifics can have on the sensitivity of ENSO to climate change. Therefore, to increase the robustness, multimodel ensembles have been used in many later studies. In a study by Merryfield (2006), 12 out of 15 models (prepared for IPCC AR4) agreed on a decrease in ENSO period. Cai et al. (2014) analysed extreme El Niño events in models that participated in Coupled Model Intercomparison Project (CMIP) Phases 3 and 5. They found that extreme El Niño events, defined based on precipitation, will occur more frequently in a changing climate, even though SST anomalies in the Niño3 region do not show a significant change. Cai et al. (2015b) carried out a similar analysis for extreme La Niña events. Based on both studies, they concluded that there is a high model consensus that both extreme La Niña and El Niño events become more frequent under climate change (Cai et al., 2014; 2015a; 2015b). Wang et al. (2017) also used 13 models participating in CMIP Phase 5 (CMIP5) and came to the same conclusion. But, many studies that investigated multimodel ensembles concluded that the predictions of ENSO frequency are strongly model-dependent. Studies by Guilyardi (2006), Deng et al. (2010), Chen et al. (2017), and Xu et al. (2017) suggest that the model consensus is very small on the topic of how ENSO frequency will change in a changing climate.

There are first studies that analyse the newest generation of climate models, participating in CMIP Phase 6 (CMIP6). Fredriksen et al. (2020) investigate the agreement of the models in this intercomparison project on projected changes of ENSO. They find that although the agreement seems improved compared to earlier phases of CMIP, there is still no consensus regarding the ENSO variance and spectra. However, they find that models agree on some signals like the decreasing strength of the east–west SST gradient or the increasing variance of SST in the Niño3.4 region. Brown et al. (2020) analyse CMIP6 models in their assessment of ENSO changes in past and future climates. They find that the models used in their study simulate ENSO patterns that resemble observations reasonably well. This study, once again, concludes that changes in ENSO variability in future simulations are highly model-dependent. Freund et al. (2020) studied frequency and intensity changes of ENSO in CMIP5 and CMIP6 models and could not find an overall agreement between models. This disagreement persists when they investigate only a subset of presumably better performing models.

The fact that many studies that concerned themselves with changes in ENSO produce very different results raises the question if there might be a reason why we cannot predict these changes. Chen *et al.* (2017) mentioned that the difficulty in predicting ENSO properties is not only the intermodel spread but also the significant natural variability and Zheng *et al.* (2018) support this hypothesis in a study about ENSO amplitude. A similar study by Maher *et al.* (2018) showed that (depending on the warming scenario) up to 90% of the variability of ENSO amplitude can be attributed to internal variability. Zheng *et al.* (2018) and Maher *et al.* (2018) stressed that the internal variability of ENSO has a high impact on the predictability of changes in amplitude and Chen *et al.* (2017) mentioned that changes in many ENSO statistics may not be significant.

We investigate this general issue further, introducing a new approach to separate natural variability and intermodel differences. We focus specifically on changes in ENSO frequency. In particular, our goal is to find out if the large uncertainty in predicted changes of ENSO frequency is mainly due to different model reactions to CO_2 forcing, or due to apparent trends resulting from a combination of natural variability and limited time series length. We use the 1%/year CO_2 increase experiment of CMIP6. Additionally, we use the unforced control experiment to quantify the role of natural variability, which is a new approach that differentiated this study from earlier work cited above.

Section 2 of this paper gives a short overview over the data used. In section 3 we describe our methods. Results are given in section 4 and section 5 contains the conclusion and discussion.

2 | DATA

Our approach requires the comparison of simulations of the same length (150 years) from a forced experiment and the pre-industrial control (piControl) experiment from CMIP6. As the forced experiment we chose the 1pctCO2 experiment, which is initialised from the control run, and a 150-year period is simulated during which the CO_2 concentration is continuously increased by 1% each year. This results in a doubling of CO_2 after about 70 years and a quadrupling after 140 years, respectively. This ensemble will be referred to as 1pct-ensemble. While this is still a quite simplistic experiment, it is closer to reality than others, for example, the abrupt quadrupling of CO_2 concentrations.

We compare the simulations from the 1pctCO2 experiment to the piControl simulations. In the piControl experiment the year 1850 is used as a reference year and

the simulations are run for at least 500 years (Eyring *et al.*, 2016). We use the last 150 years of each simulation for our analysis and will refer to them as the Control-ensemble.

For both experiments we have an ensemble of 43 members available (a list with detailed information can be found in Table S1, Supporting Information). We use monthly mean SST data in the tropical Pacific (120°E–60°W, 30°N–30°S) from both of these ensembles for the analysis.

It should be mentioned here that the goal of the study is not to prove if there is a trend in ENSO frequency in general or to find its natural variability. Rather the aim is to see if one can predict changes in ENSO frequency for the nearer future. If the former were the goals, other datasets would be more suited.

3 | METHODS

3.1 | ENSO index

Many indices can be used to measure ENSO activity, each of which has its advantages and disadvantages. Depending on the available data and the question posed, different indices prove to be helpful. In this work, we make use of an index based on the first empirical orthogonal function (EOF) of SST data from the tropical Pacific (120°E–60°W, 30°N–30°S), similar to the works of Penland and Sardeshmukh (1995), Merryfield (2006), or Berner *et al.* (2020). The pattern of the first EOF (EOF1) explains most of the variability in the tropical Pacific, particularly in the Niño3.4 region (Dommenget *et al.*, 2013). In our 43-member Control-ensemble, the explained variance of the first EOF is 47.64% on average, while the second EOF explains less than 13.87% for all members (7.85% on average). Between the Control- and 1pct-ensemble the patterns and the amount of explained variance differ only slightly. Therefore, the principal component (PC) of the first EOF can be used as an ENSO index.

We normalize the time series of the first principal component (PC1) by scaling it to unit variance, which makes the time series of different models comparable, even if they have different ENSO amplitudes. We verified that the resulting index is, in fact, highly correlated with the Ocean Nino Index (ONI) defined by NOAA Climate Prediction Center, National Weather Service (2020a) (which is defined as the field mean of SST anomalies over the Niño3.4 region, 5°N–5°S and 120°–170°W). The correlation coefficient between the PC1 and the models' ONI is 0.971 on average for the 43 models of the control experiment (min: 0.883, max: 0.991). This means that they

indeed describe the same ENSO variations (also see Penland and Sardeshmukh, 1995; Berner *et al.*, 2020). The sign of the PC is chosen in such a way that the PC time series is positively instead of negatively correlated with the ONI.

To calculate the ONI or the PC1, the climate trend and annual cycle have to be eliminated. This is done as described by NOAA Climate Prediction Center, National Weather Service (2020a) for the ONI. Anomalies are calculated for each grid point with respect to a centred base-period. This base-period is updated every 5 years to account for the warming trend in the region. The base-period corresponding to the years x to $x + 4$ is the period $x - 15$ to $x + 14$ (NOAA Climate Prediction Center, National Weather Service, 2020b), so that the 30-year base-period centred around x is valid for 5 years of which year x is the first (the base-period for the years $x + 5$ to $x + 9$ would be $x - 10$ to $x + 19$ then). Subsequently, the anomalies are smoothed by a 3-month running mean. From these smoothed anomalies EOFs and scaled PC time series can be calculated. The scaled first PC is used as the ENSO index in this study and will be referred to as the PC index. The base-period method creates artificial trends at the beginning and end of a dataset because for the first and last 15 years there is no correctly centred base-period available, so the closest possible base-period has to be used. This creates an unwanted effect, which cannot be corrected. Hence, the first and last 15 years of data cannot be correctly evaluated and will not be taken into account for further analysis. We therefore effectively analyse time series with a length of 120 years. An example of the resulting time series for an arbitrarily chosen ensemble member can be found in Figure S1.

3.2 | Analysis of ENSO frequency

The NOAA Climate Prediction Center, National Weather Service (2020a) consider a month "El Niño-like" or "La Niña-like" when the ONI exceeds ±0.5 K, respectively. The properties of ENSO in coupled climate models are not necessarily the same as the statistics of the observed phenomenon, nor do they have to be the same for different models. Therefore, a fixed threshold has a different meaning for different models. Instead, one should use a flexible threshold like one standard deviation (like, e.g., Merryfield, 2006). Because we use the normalized PC as ENSO index, the time series of the different models are indeed comparable, and a flexible threshold of one standard deviation corresponds to the fixed value of ±1 for all PC indices. According to this definition, an El Niño (EN) occurs when the PC index exceeds 1 and a La Niña (LN) occurs when the PC index goes below −1. As a measure of ENSO frequency, we use the number of ENs and LNs during 30 years. A time series of occurrences of these ENs and LNs is created by counting the months that meet the condition within a 30-year moving window. This way a time series can be achieved where the number of ENs or LNs corresponding to each month is the number of ENs or LNs within a 30-year window centred at that month.

We fit a regression line to time series resulting from the mentioned counting method. Then, we can use the slope of the regression line to evaluate if there is a change in ENSO frequency. This trend calculation via the regression line is done for each ensemble member and both experiments. Then, the average slope (m_{1pct}, $m_{Control}$) and its standard deviation over all members (σ_{1pct}, $\sigma_{Control}$) are calculated for both experiments.

The choice of the correct window length is not obvious. The shorter the window is, the bigger we can expect the standard deviation of the resulting time series to be. The longer the window is, the shorter the resulting time series gets. Both can increase the uncertainty of trends in that time series (Weatherhead *et al.*, 1998). We tested window lengths of 20, 30, and 40 years and found that the results support the same conclusions, therefore we can confidently do our analysis for the 30-year moving window.

According to the NOAA Climate Prediction Center, National Weather Service (2020a), EN or LN events are not counted until the condition is met for at least five consecutive months. This definition has the disadvantage of fewer occurrences in general and therefore a bigger statistical error. Nevertheless, the same analysis described above for EN/LN-like months can be done for these events. The results are consistent with the ones for EN/LN-like months and can be found in Supporting Information.

3.3 | Causes for uncertainty in the ENSO frequency trend estimate

The time series which can be used to predict a change in ENSO frequency in the nearer future are of limited length. For the 1pct-ensemble, this is 150 years (120 years after computing the PC index). ENSO is happening in the tropical Pacific, where variabilities on different timescales play a role. SSTs and therefore ENSO frequency can be subject to variability on scales of months, years, decades, or even centuries. The variety of variabilities and their causes exceeds the scope of this paper, but the reader is referred to literature on the topic like Zou and Latif (1994), Latif (2001), Rodgers *et al.* (2004), or Latif *et al.* (2013).

Especially with a phenomenon with large internal variability, the limited length of the time series might lead to apparent trends (see Weatherhead *et al.*, 1998). In order to illustrate this problem, we show an example here. We
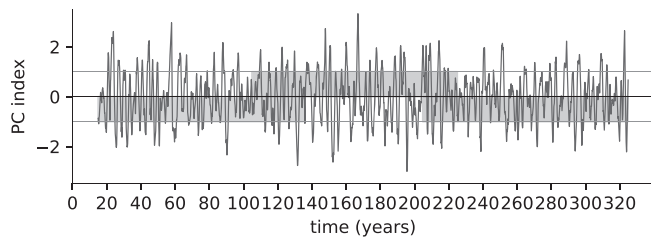
FIGURE 1 Long time series of PC index for model 29 (IPSL-CM6A-LR), based on first 340 years of piControl simulation. Different periods of 120 years are shaded in colours [Colour figure can be viewed at wileyonlinelibrary.com]
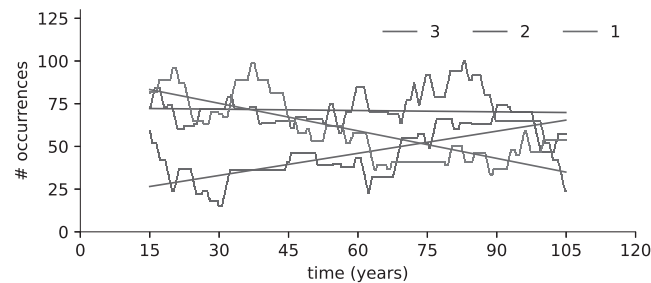

FIGURE 2 Time series of occurrences of EN like months (within a 30-year window). Calculated based on the 120-year subsets of the time series shaded in Figure 1. Model 29 (IPSL-CM6A-LR). Straight lines show linear fits [Colour figure can be viewed at wileyonlinelibrary.com]

arbitrarily chose model 29 (IPSL-CM6A-LR) to demonstrate. For this example, we use the first 340 years (also arbitrarily chosen) of the piControl experiment. This results in a time series of the PC index of 310 years. This time series can be seen in Figure 1. We would not expect any trend in ENSO frequency in the unforced run, no matter if we use the entire time series or shorter subsets of it. To show how the length and location of the time series chosen to calculate the trends influences the results nevertheless, we carry out the analysis for three different subsets of the long time series. The chosen subsets are of 120-years length, which is the maximum length we can look at for the 1pct simulations. The subsets are marked in colours in Figure 1. The resulting time series of occurrences of EN and their trends can be seen in Figure 2. It becomes obvious that the detected trends are very different. This is what we call apparent trends. This example demonstrates that these apparent trends stem only from internal variability together with the limited length of the time series. The uncertainty in the detected trends that is caused by this effect is irreducible.

In this study, we want to estimate how much of the uncertainty of detected changes in ENSO frequency is because of this fact and how much can be attributed to the different model reactions. Therefore, we need to quantify how big the standard deviations of trends are that arise

from the limitation of the forced experiment to only 150 years. We do this by analysing time series of 150 years from the piControl experiment (120 years after the index calculation). Because there is no forcing in the piControl experiment, we expect there to be no trend in ENSO frequency. Any trend that can be detected is therefore an apparent trend. From the Control-ensemble, we can therefore calculate an uncertainty in the estimated trend of ENSO frequency, which is due to apparent trends,

$$\sigma_{\text{Control}}^2 = \sigma_{\text{ApparentTrends}}^2. \tag{1}$$

Conversely, we can expect there to be a trend in the 1pct-ensemble due to CO_2 forcing. This trend now is subject to two causes of uncertainty: The different reactions of different models to the forcing ($\sigma_{\text{ModelDiff}}$), as well as apparent trends due to the limited length of the time series. It has to be noted that the uncertainty due to apparent trends does not necessarily have to be the same as in the Control-ensemble, since internal variability could have changed, too. If we assume that the two causes are uncorrelated, the uncertainty of the ENSO frequency trend estimate in the 1pct-ensemble can be written as

$$\sigma_{\text{1pct}}^2 = \sigma_{\text{ModelDiff}}^2 + \sigma_{\text{ApparentTrends}}^2 - \Delta\sigma_{\text{ApparentTrends}}^2, \tag{2}$$

where $\Delta\sigma_{\text{ApparentTrends}}^2$ is the difference between the two experiments' uncertainty due to apparent trends.

4 | RESULTS

The first empirical orthogonal function (EOF1) shows a distinct monopole pattern for all the models, which has its maximum in the eastern central Pacific (Figure S2). Although the intensity and meridional and zonal extent vary between the models, it is obvious that the patterns are similar. The pattern of the first EOF explains 47.64% of the variance for the Control-ensemble on average, and 49.58% for the 1pct-ensemble. For most of the models the explained variances are higher, with only a few exceptions. We believe that the models with low explained variance also have a less pronounced ENSO. This is supported by Figure 3, where the explained variances are depicted against the maximum amplitude of the pattern for each model. It becomes obvious that most models show an explained variance between 40 and 70%. Overall, larger amplitudes seem to be correlated with larger explained variances. All models with small explained variances (<30%) have amplitudes below 1 K. These models with a weak ENSO should be treated carefully when used to analyse changes in ENSO. We therefore conduct our
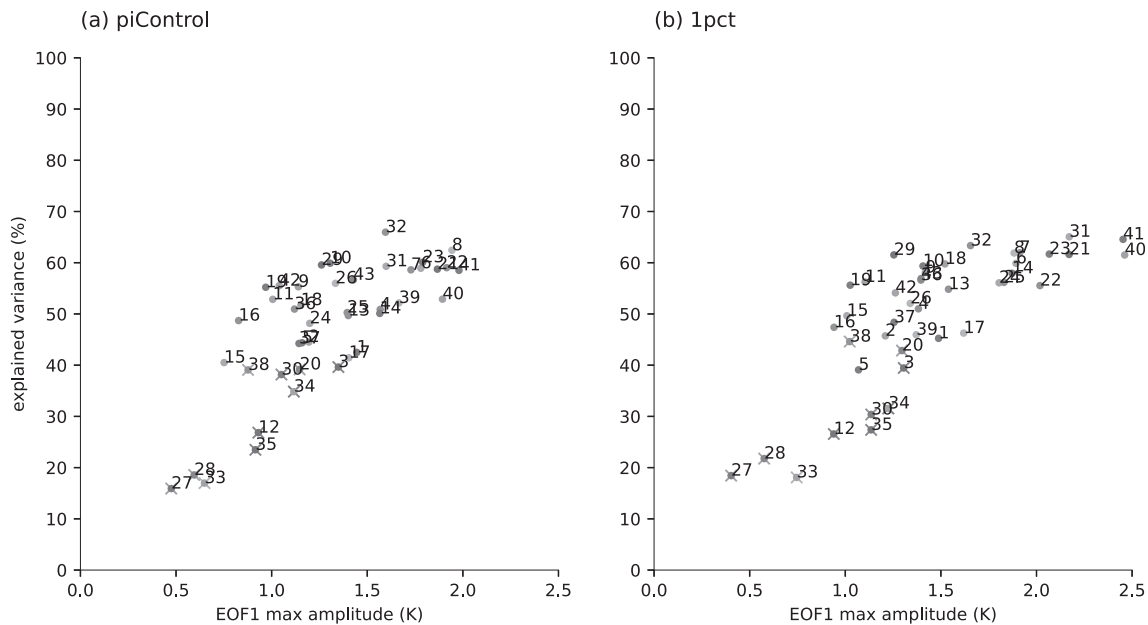
FIGURE 3 Explained variance against maximum amplitude of the EOF1 pattern for each member of the two ensembles: (a) the Control-ensemble, (b) the 1pct-ensemble. Numbers in panels (a, b) correspond to models as in Table S1. Models excluded for the reduced ensemble are shown as crosses [Colour figure can be viewed at wileyonlinelibrary.com]

analysis twice, once for the entire ensemble, once with a reduced ensemble. In the reduced ensemble we excluded all models that have less than 40% explained variance in their EOF1 of the piControl experiment (models numbers 3, 12, 20, 27, 28, 30, 33, 34, 35, and 38, as in Table S1). The EOF1 patterns for all ensemble members and both ensembles can be found in Figures S2 and S3.

If one compares the patterns of the piControl experiment to the 1pctCO2 experiment, it becomes obvious that the patterns do not change by much, in fact the pattern correlation is 0.97 on average (0.99 when excluding the 10 models mentioned above). The high pattern correlation suggests that the ENSO pattern does not change much under increased CO_2, so that the trend-variability estimated from the Control-ensemble can be transferred to the 1pct-ensemble. For some models, the EOF spatial pattern seems to change more than for others. This is consistent with the literature suggesting that ENSO might change to a more central Pacific than eastern Pacific pattern (e.g., Yeh et al., 2009), although Xu et al. (2017) find poor model consensus on this topic.

As a measure of ENSO frequency we use the number of occurrences of El Niño-like and La Niña-like months within a moving 30-year time window (=30 yearly events). The average number of occurrences over all 30-year-windows for each model is depicted in Figure 4. It seems as if in panel (b), showing the 1pct-ensemble, the number of El Niños (ENs) and La Niñas (LNs) is better correlated. This shows that there are indeed changes in ENSO frequency under forcing for some models. The

changes seem to be correlated, since models that predict more frequent EN also predict more frequent LN. However, this picture is strongly dominated by only three models (30, 21, 23). If they are removed the variability cloud looks similar to the control experiment.

To analyse the mean change in the frequency of EN and LN events, we fit regression lines to the time series of occurrences for each member (see section 3.2). The ensemble mean of the slopes of the regression lines can be interpreted as a measure for the mean change of ENSO frequency in that ensemble. Figures 5 and 6 show the time series of occurrences of EN and LN, respectively, for the 1pctCO2 experiment for two randomly chosen ensemble members and the ensemble mean. This linear trend is expressed as the gradient in events per 30-year-window/month. To convert this into a more convenient and intuitive measure for the change in ENSO frequency, we multiplied this value by 120 months, which gives the change in the number of occurrences per 30-year-window during one decade. If there are x EN-like months within the 30-year-window centred at time t and the trend was 2, then there are $x + 2$ EN-like months within the 30-year-window centred at $t + 10$ years. The trends for all models are depicted in Figure 7. It can be seen that the different models yield quite different results. Because the different models have a different mean ENSO frequency (see Figure 4), one might argue that it is more informative to look at the relative change in events instead of the absolute change. This is depicted in Figure 8. It becomes obvious that the difference is marginal.
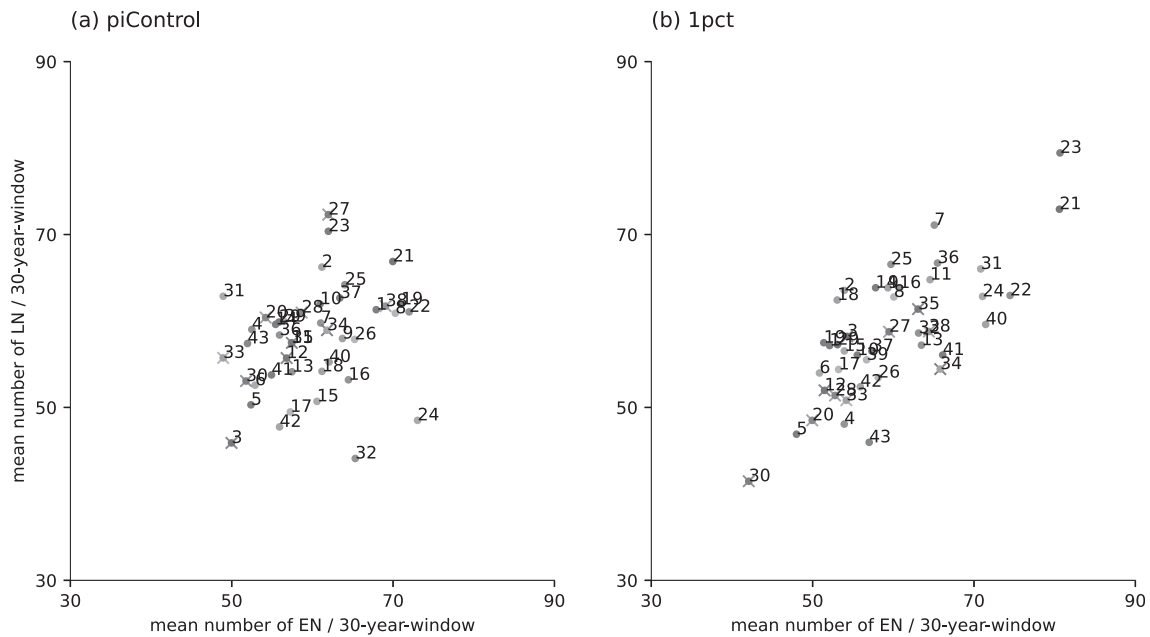
(a) piControl

(b) 1pct

FIGURE 4 Average number of El Niño/La Niña-like months for each member of the two ensembles: (a) the Control-ensemble, (b) the 1pct-ensemble. Numbers in panels (a, b) correspond to models as in Table S1. Models excluded for the reduced ensemble are shown as crosses [Colour figure can be viewed at wileyonlinelibrary.com]
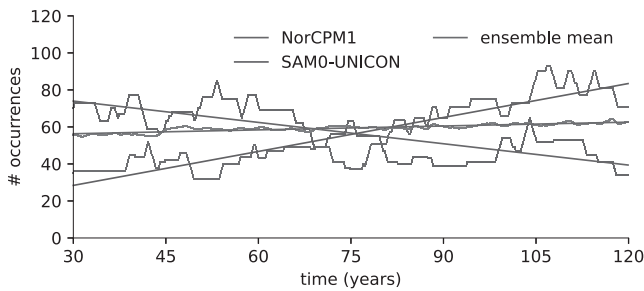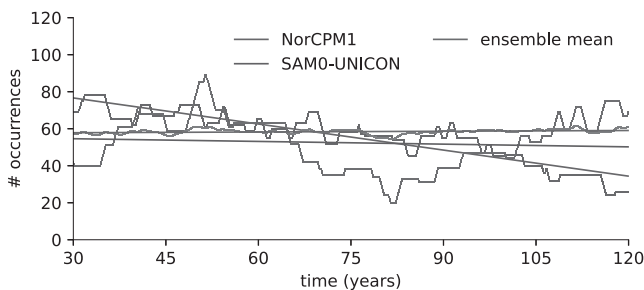

FIGURE 5 Time series of occurrences of EN like months (within a 30-year window) for the 1pct-ensemble. Blue: model 39 (NorCPM1), green: model 42 (SAM0-UNICON), red: ensemble mean. Straight lines show linear fits [Colour figure can be viewed at wileyonlinelibrary.com]

FIGURE 6 Time series of occurrences of LN like months (within a 30-year window) for the 1pct-ensemble. Blue: model 39 (NorCPM1), green: model 42 (SAM0-UNICON), red: ensemble mean. Straight lines show linear fits [Colour figure can be viewed at wileyonlinelibrary.com]

The results for the entire ensemble are summarized in Table 1. Table 2 shows the same results for the reduced ensemble. As described earlier we would expect no change at all in the control climate due to a lack of forcing. We see from the Control-ensemble that in the ensemble average there is a slight decrease of both El Niño and La Niña frequency, although it is still quite close to the expected trend of zero with a change of -0.15 ± 0.36 and -0.25 ± 0.37 30-yearly events per decade for EN and LN, respectively (mean $m \pm$ standard error $\sigma/\sqrt{N}$, where N is the number of models; see Table 1). The small trend that we do detect is due to the finite size of the ensemble (so the apparent trends of individual members are not averaged out entirely). Also, the standard deviations are relatively large with 2.3 and 2.4 30-yearly events per decade, which is one order of magnitude bigger than the mean trend itself. This is therefore the uncertainty that stems from only using 150-year time series for the analysis. The mean over the 1pct-ensemble on the other hand shows a slight increase in frequency with 0.70 ± 0.47 and 0.13 ± 0.40 more 30-yearly events per decade for EN and LN, respectively. The standard deviations are 3.0 and 2.6 30-yearly events per decade, therefore they are again one order of magnitude bigger than the mean change itself.

The results for the reduced ensemble look very similar, although with a slight reduction in all mean values but a bigger standard error: We find a change of -0.34 ± 0.42 and -0.30 ± 0.42 in EN and LN frequency in the Control-
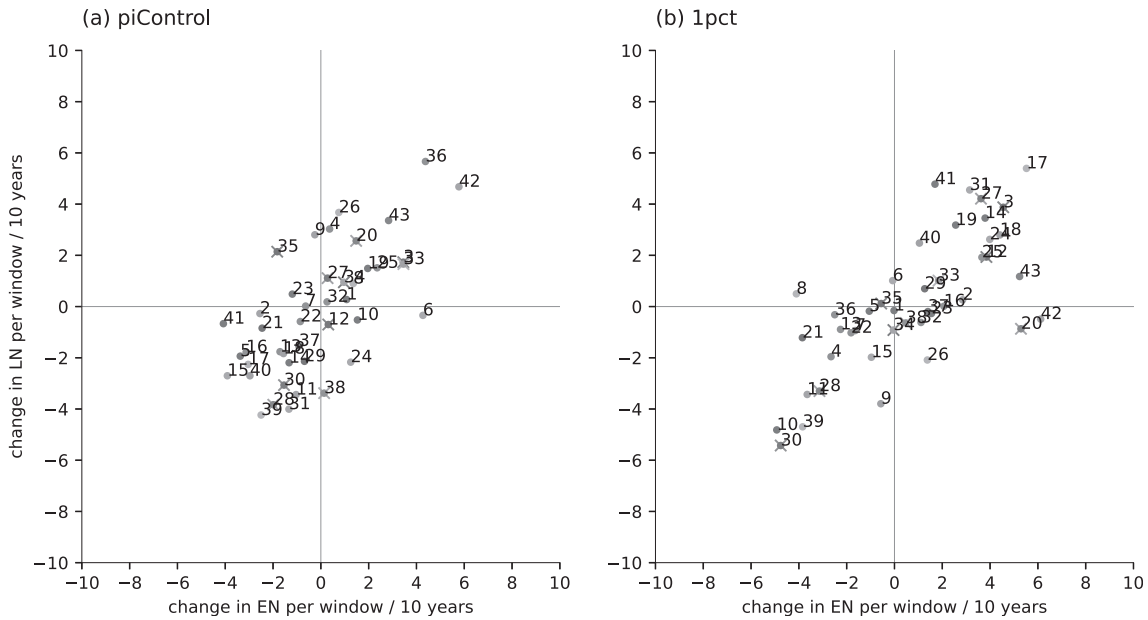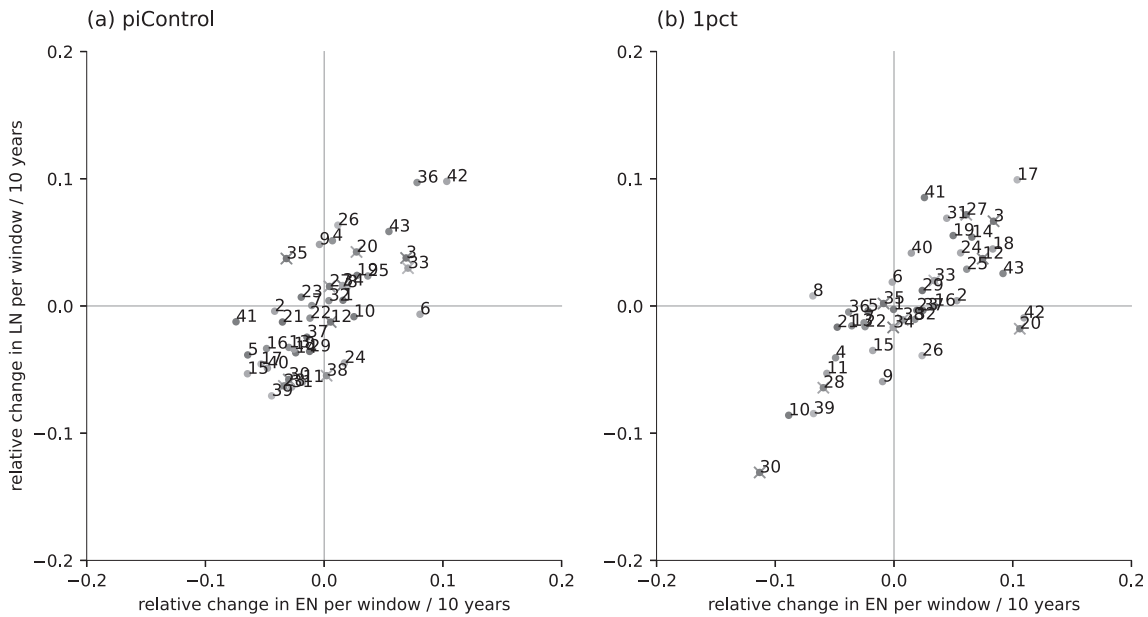
FIGURE 7 Linear trend in El Niño/La Niña-like months for each member of the two ensembles: (a) the Control-ensemble, (b) the 1pct-ensemble. The unit has been transformed from gradient in (occurrences per 30-year-window/month) into the more intuitive measure of additional events per 30-year-window in 10 years by multiplying the gradient by 120 months. A value of 0.5 means that there will be half an additional event per 30-year-window in 10 years. Numbers in panels (a, b) correspond to models as in Table S1 [Colour figure can be viewed at wileyonlinelibrary.com]

FIGURE 8 Relative linear trend in El Niño/La Niña-like months for each member of the two ensembles: (a) the Control-ensemble, (b) the 1pct-ensemble. Absolute numbers of occurrences in EN/LN have been divided by the mean value of the respective models, to create a time series of relative number of occurrences before calculating the trends. Numbers in panels (a, b) correspond to models as in Table S1 [Colour figure can be viewed at wileyonlinelibrary.com]

	El Niños		La Niñas	
	$m \pm \sigma/\sqrt{N}$	σ	$m \pm \sigma/\sqrt{N}$	σ
piControl	−0.1544 ± 0.3569	2.3403	−0.2488 ± 0.3685	2.4167
1pct	0.6974 ± 0.4671	3.0627	0.1341 ± 0.3962	2.5978

TABLE 1 Means (m) and standard deviations (σ) of predicted changes in occurrences of El Niños and La Niñas (units are #/month*120 months)

	El Niños		La Niñas	
	$m \pm \sigma/\sqrt{N_{\mathrm{reduced}}}$	σ	$m \pm \sigma/\sqrt{N_{\mathrm{reduced}}}$	σ
piControl	-0.3441 ± 0.424	2.4359	-0.299 ± 0.424	2.4358
1pct	0.5716 ± 0.5252	3.0171	0.1748 ± 0.4392	2.523

ensemble. In the 1pct-ensemble the trends are 0.57 ± 0.53 and 0.17 ± 0.44 for EN and LN, respectively.

5 | DISCUSSION AND CONCLUSION

We hypothesise that natural variability is too big (or the trend too small) to reliably detect a trend in ENSO frequency for the nearer future (e.g., 150 years) in a scenario with reasonable changes in CO_2 concentration. From the trends presented in section 4 (Tables 1 and 2), it seems like there is a slight increase in El Niños and La Niñas in the future scenario. The question is, however, how important this small change is, considering the large uncertainty. We want to answer the question if the large uncertainties can be reduced to improve the estimate of ENSO frequency trends. This would be the case if the uncertainty in the forced model is dominated by $\sigma_{\mathrm{ModelDiff}}$ because this can be reduced by improving the models. From Tables 1 and 2 one can see that the standard deviation in the forced ensembles is big (compared to the mean change). However, it is also big in the unforced ensembles. We would expect that the standard deviation of the forced ensembles are increased compared to the unforced ensembles, due to the uncertainty introduced by model differences (see also Equation (2)). The increase is relatively small though, which can be seen to imply that the uncertainty due to apparent trends dominates and the uncertainty due to model differences plays a subordinate role.

We now want to quantify these uncertainties. Since there is no way to calculate $\sigma_{\mathrm{ModelDiff}}^2$ or $\Delta\sigma_{\mathrm{ApparentTrends}}^2$ directly, assumptions have to be made. If we assume for a moment that the natural variability of ENSO does not change under climate change, and therefore the uncertainty due to apparent trends stays the same ($\Delta\sigma_{\mathrm{ApparentTrends}}^2 = 0$, and still under the assumptions that the uncertainties are uncorrelated), we get an estimate of the remaining uncertainty, which is caused by different reactions of the models to the forcing,

$$\sigma_{\mathrm{ModelDiff}}^2 = \sigma_{\mathrm{1pct}}^2 - \sigma_{\mathrm{ApparentTrends}}^2 = \sigma_{\mathrm{1pct}}^2 - \sigma_{\mathrm{Control}}^2. \quad (3)$$

For the entire ensemble, the resulting standard deviations due to model differences are calculated as

$$\sigma_{\mathrm{ModelDiff}}(\mathrm{EN}) = \sqrt{3.0627^2 - 2.3403^2} = 1.9756, \quad (4)$$

$$\sigma_{\mathrm{ModelDiff}}(\mathrm{LN}) = \sqrt{2.5978^2 - 2.4167^2} = 0.9529. \quad (5)$$

The uncertainty caused by model differences is still one order of magnitude larger than the mean changes, but it is also smaller than the uncertainty due to apparent trends ($\sigma_{\mathrm{Control}} = \sigma_{\mathrm{ApparentTrends}}$). This means that the greater part of the uncertainty actually stems from apparent trends and can therefore not be reduced. The same conclusion holds for the reduced ensemble, where $\sigma_{\mathrm{ModelDiff}}(\mathrm{EN}) = 1.7802$ and $\sigma_{\mathrm{ModelDiff}}(\mathrm{LN}) = 0.6576$.

Obviously, the assumption made is a very strict one. It is very well possible that the natural variability of the system changes, so that the apparent trends and the resulting uncertainty change. We want to estimate by how much the uncertainty due to apparent trends could reduce before the conclusion would no longer be valid because it no longer dominates. Therefore, we now allow $\Delta\sigma_{\mathrm{ApparentTrends}}^2$ to be positive, which represents a reduction of $\sigma_{\mathrm{ApparentTrends}}^2$ in the future climate. We focus only on the case where $\sigma_{\mathrm{ApparentTrends}}^2$ is reduced because this would potentially invalidate our conclusion. Our conclusion would only change if $(\sigma_{\mathrm{ApparentTrends}}^2 - \Delta\sigma_{\mathrm{ApparentTrends}}^2)$ does not dominate σ_{1pct}^2 anymore, and therefore is of the same size as $\sigma_{\mathrm{ModelDiff}}^2$ or smaller. This is the case, when $(\sigma_{\mathrm{ApparentTrends}}^2 - \Delta\sigma_{\mathrm{ApparentTrends}}^2)$ makes up less than half of σ_{1pct}^2. The tipping point can therefore be calculated as

$$\frac{1}{2}\sigma_{\mathrm{1pct}}^2 = \sigma_{\mathrm{ApparentTrends}}^2 - \Delta\sigma_{\mathrm{ApparentTrends}}^2, \quad (6)$$

$$\Delta\sigma_{\mathrm{ApparentTrends}}^2 = \sigma_{\mathrm{ApparentTrends}}^2 - \frac{1}{2}\sigma_{\mathrm{1pct}}^2, \quad (7)$$

$$= \sigma_{\mathrm{Control}}^2 - \frac{1}{2}\sigma_{\mathrm{1pct}}^2. \quad (8)$$

For EN this means that $\sigma_{\mathrm{ApparentTrends}}^2$ has to be reduced by 0.7869, which means a decrease of 14.4%. For LN the change would even have to be 2.4662, which is 42.2% of the present value. In the reduced ensemble, the values are 23.3% and 30.2% for EN and LN, respectively. These numbers are also a little bit sensitive to the chosen moving-window, but the results are in general

agreement. According to Weatherhead *et al.* (1998) the uncertainty introduced by a time series of limited length ($\sigma^2_{\text{ApparentTrends}}$ in our case) is dependent on the magnitude and the autocorrelation of the noise in the data of a given length. This means that for $\sigma^2_{\text{ApparentTrends}}$ to decrease significantly, either the magnitude and/or the autocorrelation of the noise in the time series of occurrences of EN and LN have to decrease significantly. While it is difficult to say how much change is likely to happen, this analysis gives an idea of the problem. The changes needed to invalidate our conclusion are relatively big for the LN case, which indicates that it is very difficult to predict if LN frequency changes in a future scenario. For the EN cases the picture is not so clear, changes to the natural variability do not have to be so big to change our conclusion. Nevertheless, even if the uncertainty due to apparent trends would not dominate anymore, it would still be responsible for a large part of the uncertainty, severely limiting the scope for improving EN frequency prediction by model improvements.

A major goal of current research is to predict how ENSO behaviour will change under a changing climate. In this study, we focused on the prediction of ENSO frequency changes for the nearer future. For this purpose, the 43-member CMIP6 1pct-ensemble and Control-ensemble were analysed. Uncertainties about the future change of ENSO frequency arise because ENSO is a phenomenon with high internal variability and the time series are of limited length so that apparent trends can appear. We assumed that the uncertainties stemming from apparent trends and different model reactions are uncorrelated. Then, we could use 150 years of the piControl simulations to find how big the uncertainty caused by these apparent trends is, and we could subtract this result from the result for the 1pct-ensemble, to find the uncertainty caused by different model reactions. We can conclude that, unless the uncertainty due to apparent trends reduces by more than 14.4% (23.3% in the reduced ensemble) in the forced experiment relative to piControl, it dominates the uncertainty of the ENSO frequency trend estimate. This means that the major part of the uncertainty is irreducible, which makes it very difficult to estimate changes in ENSO frequency on a timescale of 150 years.

DATA AVAILABILITY STATEMENT

All CMIP6 data used in this work are made available by the DKRZ (Deutsches Klimarechenzentrum). Scripts used to process and analyse the data can be found here: https://doi.org/10.5281/zenodo.6841964.

ORCID

Fiona Fix https://orcid.org/0000-0002-0413-6090
Stefan A. Buehler https://orcid.org/0000-0001-6389-1160

REFERENCES

Aiken, C.M., Santoso, A., McGregor, S. and England, M.H. (2013) The 1970's shift in enso dynamics: a linear inverse model perspective. *Geophysical Research Letters*, 40(8), 1612–1617. https://doi.org/10.1002/grl.50264.

Berner, J., Christensen, H.M. and Sardeshmukh, P.D. (2020) Does ENSO regularity increase in a warming Climate? *Journal of Climate*, 33(4), 1247–1259.

Brown, J.R., Brierley, C.M., An, S.-I., Guarino, M.-V., Stevenson, S., Williams, C.J.R., Zhang, Q., Zhao, A., Abe-Ouchi, A., Braconnot, P., Brady, E.C., Chandan, D., D'Agostino, R., Guo, C., LeGrande, A.N., Lohmann, G., Morozova, P.A., Ohgaito, R., O'ishi, R., Otto-Bliesner, B.L., Peltier, W.R., Shi, X., Sime, L., Volodin, E.M., Zhang, Z. and Zheng, W. (2020) Comparison of past and future simulations of ENSO in CMIP5/PMIP3 and CMIP6/PMIP4 models. *Climate of the Past*, 16(5), 1777–1805. https://doi.org/10.5194/cp-16-1777-2020.

Cai, W., Borlace, S., Lengaigne, M., Rensch, P., Collins, M., Vecchi, G., Timmermann, A., Santoso, A., McPhaden, M., Wu, L., England, M., Wang, G., Guilyardi, E. and Jin, F.-F. (2014) Increasing frequency of extreme El Nino events due to greenhouse warming. *Nature Climate Change*, 4, 111–116. https://doi.org/10.1038/nclimate2100.

Cai, W., Santoso, A., Wang, G., Yeh, S.-W., An, S.-I., Cobb, K.M., Collins, M., Guilyardi, E., Jin, F.-F., Kug, J.-S., Lengaigne, M., McPhaden, M.J., Takahashi, K., Timmermann, A., Vecchi, G., Watanabe, M. and Wu, L. (2015a) ENSO and greenhouse warming. *Nature Climate Change*, 5, 849–859. https://doi.org/10.1038/nclimate2743.

Cai, W., Wang, G., Santoso, A., McPhaden, M., Lixin, W., Jin, F.-F., Axel Timmermann, M., Collins, G.V., Lengaigne, M., England, M., Dommenget, D., Takahashi, K. and Guilyardi, E. (2015b) Increased frequency of extreme La Niña events under greenhouse warming. *Nature Climate Change*, 5, 132–137. https://doi.org/10.1038/nclimate2492.

Chen, C., Cane, M.A., Wittenberg, A.T. and Chen, D. (2017) ENSO in the CMIP5 simulations: life cycles, diversity, and responses to Climate change. *Journal of Climate*, 30(2), 775–801. https://doi.org/10.1175/JCLI-D-15-0901.1.

Collins, M. (2000a) Understanding uncertainties in the response of ENSO to greenhouse warming. *Geophysical Research Letters*, 27(21), 3509–3512. https://doi.org/10.1029/2000GL011747.

Collins, M. (2000b) The El Niño–Southern Oscillation in the second Hadley Centre coupled model and its response to greenhouse warming. *Journal of Climate*, 13(7), 1299–1312. https://doi.org/10.1175/1520-0442(2000)013<1299:TENOSO>2.0.CO;2.

Dawson, A. (2016) eofs: a library for EOF analysis of meteorological, oceanographic and climate data. *Journal of Open Research Software*, 4(1), e14. https://doi.org/10.5334/jors.122.

Dommenget, D., Bayr, T. and Frauen, C. (2013) Analysis of the non-linearity in the pattern and time evolution of El Niño Southern Oscillation. *Climate Dynamics*, 40, 2825–2847. https://doi.org/10.1007/s00382-012-1475-0.

Eyring, V., Bony, S., Meehl, G.A., Senior, C.A., Stevens, B., Stouffer, R.J. and Taylor, K.E. (2016) Overview of the Coupled Model Intercomparison Project phase 6 (CMIP6) experimental design and organization. *Geoscientific Model Development*, 9(5), 1937–1958. https://doi.org/10.5194/gmd-9-1937-2016.

Fredriksen, H.-B., Berner, J., Subramanian, A.C. and Capotondi, A. (2020) How does El Niño–Southern Oscillation change under global warming—a first look at CMIP6. *Geophysical Research Letters*, 47(22), e2020GL090640. https://doi.org/10.1029/2020GL090640.

Freund, M.B., Brown, J.R., Henley, B.J., Karoly, D.J. and Brown, J.N. (2020) Warming patterns affect el niño diversity in CMIP5 and CMIP6 models. *Journal of Climate*, 33(19), 8237–8260. https://doi.org/10.1175/JCLI-D-19-0890.1.

Guilyardi, E. (2006) El Niño–mean state–seasonal cycle interactions in a multi-model ensemble. *Climate Dynamics*, 26, 329–348. https://doi.org/10.1007/s00382-005-0084-6.

Xu, K., Tam, C.-Y., Zhu, C., Liu, B. and Wang, W. (2017) CMIP5 projections of two types of El Niño and their related tropical precipitation in the twenty-first century. *Journal of Climate*, 30(3), 849–864. https://doi.org/10.1175/JCLI-D-16-0413.1.

Kestin, T.S., Karoly, D.J., Yano, J.-I. and Rayner, N.A. (1998) Time? Frequency variability of ENSO and stochastic simulations. *Journal of Climate*, 11(9), 2258–2272. https://doi.org/10.1175/1520-0442(1998)011<2258:TFVOEA>2.0.CO;2.

Latif, M. (2001) Tropical Pacific/Atlantic Ocean interactions at multi-decadal time scales. *Geophysical Research Letters*, 28(3), 539–542. https://doi.org/10.1029/2000GL011837.

Latif, M., Martin, T. and Park, W. (2013) Southern Ocean sector centennial climate variability and recent decadal trends. *Journal of Climate*, 26(19), 7767–7782. https://doi.org/10.1175/JCLI-D-12-00281.1.

Deng, L., Yang, X.Q. and Xie, Q. (2010) ENSO frequency change in coupled climate models as response to the increasing CO_2 concentration. *Chinese Science Bulletin*, 55, 744–751. https://doi.org/10.1007/s11434-009-0491-x.

Maher, N., Matei, D., Milinski, S. and Marotzke, J. (2018) ENSO change in climate projections: forced response or internal variability? *Geophysical Research Letters*, 45(20), 11390–11398. https://doi.org/10.1029/2018GL079764.

Merryfield, W.J. (2006) Changes to ENSO under CO_2 doubling in a multimodel ensemble. *Journal of Climate*, 19(16), 4009–4027. https://doi.org/10.1175/JCLI3834.1.

NOAA Climate Prediction Center, National Weather Service. (2020a) *Cold & warm episodes by season*. Available at: https://origin.cpc.ncep.noaa.gov/products/analysis_monitoring/ensostuff/ONI_v5.php [Accessed on 22nd March 2021].

NOAA Climate Prediction Center, National Weather Service. (2020b) *Description of Changes to Ocean Niño Index (ONI)*. Available at: https://origin.cpc.ncep.noaa.gov/products/analysis_monitoring/ensostuff/ONI_change.shtml [Accessed on 22nd March 2021].

Penland, C. and Sardeshmukh, P.D. (1995) The optimal growth of tropical sea surface temperature anomalies. *Journal of Climate*, 8(8), 1999–2024. https://doi.org/10.1175/1520-0442(1995)008<1999:TOGOTS>2.0.CO;2.

Rodgers, K.B., Friederichs, P. and Latif, M. (2004) Tropical Pacific decadal variability and its relation to decadal modulations of enso. *Journal of Climate*, 17(19), 3761–3774. https://doi.org/10.1175/1520-0442(2004)017<3761:TPDVAI>2.0.CO;2.

Timmermann, A., Oberhuber, J., Bacher, A., Esch, M., Latif, M. and Roeckner, E. (1999) Increased El Niño frequency in a climate model forced by future greenhouse warming. *Nature*, 398, 694–697. https://doi.org/10.1038/19505.

Timmermann, A. (2001) Changes of ENSO stability due to greenhouse warming. *Geophysical Research Letters*, 28(10), 2061–2064. https://doi.org/10.1029/2001GL012879.

Wang, B. and An, S.-I. (2001) Why the properties of el nino changed during the late 1970 s. *Geophysical Research Letters*, 28, 3709–3712. https://doi.org/10.1029/2001GL012862.

Wang, G., Cai, W., Gan, B., Lixin, W., Santoso, A., Lin, X., Chen, Z. and McPhaden, M.J. (2017) Continued increase of extreme El Niño frequency long after 1.5°C warming stabilization. *Nature Climate Change*, 7(8), 568–572. https://doi.org/10.1038/nclimate3351.

Weatherhead, E.C., Reinsel, G.C., Tiao, G.C., Meng, X.-L., Choi, D., Cheang, W.-K., Keller, T., DeLuisi, J., Wuebbles, D.J., Kerr, J.B., Miller, A.J., Oltmans, S.J. and Frederick, J.E. (1998) Factors affecting the detection of trends: statistical considerations and applications to environmental data. *Journal of Geophysical Research: Atmospheres*, 103(D14), 17149–17161. https://doi.org/10.1029/98JD00995.

Yang, H., Zhang, Q., Zhong, Y., Vavrus, S. and Liu, Z. (2005) How does extratropical warming affect ENSO? *Geophysical Research Letters*, 32(1), L01702. https://doi.org/10.1029/2004GL021624.

Yeh, S.-W., Kug, J.-S., Dewitte, B., Kwon, M.-H., Kirtman, B.P. and Jin, F.-F. (2009) El Niño in a changing climate. *Nature*, 461, 511–514. https://doi.org/10.1038/nature08316.

Zelle, H., Jan, G., van Oldenborgh, G.B. and Dijkstra, H. (2005) El Niño and greenhouse warming: results from ensemble

simulations with the NCAR CCSM. *Journal of Climate*, 18(22), 4669–4683. https://doi.org/10.1175/JCLI3574.1.

Zhang, Q., Guan, Y. and Yang, H. (2008) ENSO amplitude change in observation and coupled models. *Advances in Atmospheric Sciences*, 25, 361–366. https://doi.org/10.1007/s00376-008-0361-5.

Zheng, X.-T., Hui, C. and Yeh, S.-W. (2018) Response of ENSO amplitude to global warming in CESM large ensemble: uncertainty due to internal variability. *Climate Dynamics*, 50(11), 4019–4035. https://doi.org/10.1007/s00382-017-3859-7.

Zou, J. and Latif, M. (1994) Modes of ocean variability in the tropical pacific as derived from geosat altimetry. *Journal of Geophysical Research: Oceans*, 99(C5), 9963–9975. https://doi.org/10.1029/94JC00172.

SUPPORTING INFORMATION

Additional supporting information can be found online in the Supporting Information section at the end of this article.